The Astronomical Journal, 160:13 (8pp), 2020 July https://doi.org/10.3847/1538-3881/ab9094

KR Persei, a Mid-F Eclipsing Binary with a One-day Period

James R. Sowell[1], Emily Hollingworth[1], Francis C. Fekel[2], Matthew W. Muterspaugh[3,5], Horace Dale[4], Alexander D. Savello[4], Jeffrey L. Coughlin[4], and Richard M. Williamon[4]
[1] School of Physics, Georgia Institute of Technology, Atlanta, GA 30332, USA; jim.sowell@physics.gatech.edu
[2] Center of Excellence in Information Systems, Tennessee State University, 3500 John A. Merritt Boulevard, Box 9501, Nashville, TN 37209, USA fekel@evans.tsuniv.edu
[3] Fairborn Observatory, 1327 Duquesne Road, Patagonia, AZ 85624, USA; astroprofm@gmail.com
[4] Department of Physics, Emory University, Atlanta, GA 30322, USA
Received 2019 October 29; revised 2020 April 25; accepted 2020 May 3; published 2020 June 10

Abstract

KR Per is a partially eclipsing binary with an orbital period of 0.9960798 days, very close to one sidereal day, making it difficult to obtain extensive phase coverage in a reasonable amount of time. We used the Wilson–Devinney program to determine its orbital elements and stellar absolute dimensions from recently acquired radial velocities and differential *BVRI* observations that were supplemented with previous differential *UBV* measurements and published times of minima. The two components are each F5 V stars with masses of $1.466 \pm 0.015\ M_{\odot}$ and $1.458 \pm 0.015\ M_{\odot}$. The radii are $1.855 \pm 0.021\ R_{\odot}$ and $1.824 \pm 0.022\ R_{\odot}$. The orbital period of the eclipsing system is variable and more times of minima observations are needed. A comparison with evolutionary tracks indicates that the system has an age of 2.1 ± 0.1 Gyr.

Unified Astronomy Thesaurus concepts: Eclipsing binary stars (444); Spectroscopic binary stars (1557); Detached binary stars (375); Fundamental parameters of stars (555)

Supporting material: machine-readable tables

1. Introduction

KR Per = BD +43 1020 = TYC 2892-1828-1 = Gaia DR2 252670903098511360 ($\alpha = 04^{h}37^{m}08\overset{s}{.}911$, $\delta = +44°12'39\overset{''}{.}81$(2000)) is a short-period, partially eclipsing binary consisting of two mid-F main-sequence stars. The system has not been as extensively studied as many other short-period eclipsing systems because its orbital period is almost exactly one sidereal day. Chen et al. (1985) conducted a coordinated photometric campaign with observations acquired by astronomers at Yunnan Observatory, Kunming, China and by R. M. Williamon at the Fernbank Observatory in Atlanta, Georgia. At each observatory one of the two eclipses of KR Per was monitored. Chen et al. (1985) provided a brief history of the binary, and from their *UBV* data and times of minimum in the literature, they obtained a solution of its light curves based on the Russell–Merrill model (Russell & Merrill 1952; Kallrath & Milone 2009). They concluded that the system was detached and had very similar components with a combined spectral type of F5 V. Since the analysis of Chen et al. (1985), times of minima have occasionally been reported in the literature by a variety of observers.

To improve the results of Chen et al. (1985), we began a photometric campaign in 2006 at Emory University Observatory and acquired differential *BVRI* data of both eclipses as well as the phase interval from primary to secondary eclipse. In addition, starting in 2017, we obtained spectra at Fairborn Observatory in southeast Arizona and measured radial velocities of both stars. The double-lined spectra are reasonably well distributed in phase.

2. Spectroscopic Observations and Reductions

Between 2017 February and 2019 January we acquired a total of 93 useful spectroscopic observations of KR Per at Fairborn Observatory in southeast Arizona near Washington Camp (Eaton & Williamson 2004). To obtain the spectra we used the Tennessee State University 2 m Automatic Spectroscopic Telescope (AST) and a fiber-fed echelle spectrograph (Eaton & Williamson 2007). Our detector was a SITe CCD that has a 4096×4096 array of 15 μm pixels. The size of the array results in a wavelength coverage that ranges from 3800 to 8600 Å. Because of the faintness of the system, we used our largest diameter fiber, which produces a resolution of 0.4 Å, corresponding to a resolving power of 15,000 at 6000 Å. The best spectra have signal-to-noise ratios of about 50.

Fekel et al. (2009) have provided a general description of the typical velocity reduction. Specifically, for KR Per we used a solar line list that contains 168 mostly neutral Fe lines in the spectral region of 4920–7100 Å. The individual lines were fitted with a rotational broadening function (Fekel & Griffin 2011; Lacy & Fekel 2011). Unpublished velocities that were obtained with the AST, its echelle spectrograph, and the SITe CCD for several IAU solar-type velocity standard stars show that our velocities have a -0.6 km s^{-1} shift relative to the results of Scarfe (2010), so we have added 0.6 km s^{-1} to all our velocities. Our AST spectroscopic observations of KR Per are listed in Table 1.

Rotational broadening fits of the stellar lines in 16 of our best spectra provide $v \sin i$ values of 92 ± 3 km s^{-1} for both the primary and secondary.

3. Spectroscopic Orbit

For KR Per we initially adopted a period of 0.996084 days (Chen et al. 1985) and obtained spectroscopic solutions of each component with the computer program BISP (Wolfe et al. 1967).

[5] Current Address: Division of Science, Technology, and Mathematics, Columbia State Community College, 1665 Hampshire Pike, Columbia, TN 38401, USA.

Table 1
Radial Velocity Observations of KR Per

Hel. Julian Date HJD−2,400,000	Phase	RV_1 (km s^{-1})	$(O-C)_1$ (km s^{-1})	RV_2 (km s^{-1})	$(O-C)_2$ (km s^{-1})
57785.7441	0.3889	−119.0	5.1	109.0	3.3
57794.7499	0.4302	−146.0	−1.1	130.1	3.4
57795.8122	0.4967	−164.4	−5.4	150.7	9.8
57800.6624	0.3660	−104.2	5.0	89.6	−1.0
57806.7750	0.5027	−158.6	0.4	143.2	2.3
57807.7217	0.4531	−159.5	−6.9	129.2	−5.2
57813.7011	0.4560	−149.0	4.4	138.5	3.3
57814.7210	0.4799	−162.0	−4.2	142.2	2.5
57819.6806	0.4591	−159.3	−5.2	139.7	3.7
57982.9521	0.3734	−115.1	−0.8	89.4	−6.3

Note. The fractional phases and the observed minus calculated ($O-C$) residuals are from the spectroscopic solution.

(This table is available in its entirety in machine-readable form.)

We then refined those elements with SB1 (Barker et al. 1967). The separate solutions had orbital eccentricities of less than 0.02 for both components. With an orbital period of just one day, KR Per would be expected to have circularized its orbit quickly (Zahn 1977; Hut 1981; Duquennoy & Mayor 1991). Thus, we next adopted a circular orbit, allowed the period to vary, assigned unit weight to each velocity, and obtained a simultaneous solution of both components with SB2C (D. Barlow 1998, private communication). That program iterates sine/cosine fits by differential corrections to obtain a least-squares solution. The resulting period is 0.9960780 ± 0.0000029 days, which is in good agreement with the period of 0.996084 ± 0.000004 days from the photometry of Chen et al. (1985). The phases of the velocities and orbital residuals from the spectroscopic solution are given in Table 1. The resulting orbital elements and related quantities are listed in Table 2. In that table, T_0 is a time of maximum radial velocity of the primary, which occurs 0.25 in phase before primary eclipse. The minimum masses are nearly identical. Figure 1 compares the observed radial velocities and the predicted velocity curve.

4. Photometric Observations and Reductions

Our differential *BVRI* measurements were obtained with a CCD detector on the 0.6 m Emory University telescope. There were three observing nights in 2006, three nights in 2010, and one in 2011. The pre-2011 data were obtained with an Apogee AP47 CCD camera cooled to −30° C while the data in 2011 were collected with an SBIG STl0 XME CCD chip cooled to −25° C. We obtained more than 375 observations with the *BVR* filters, whereas there were 140 measurements with the *I* filter. The comparison and check stars were GSC 2892-1153 and GSC 2892-1590, respectively. The data were reduced with the standard procedures and equations from Hardie (1962). The Δ*BVRI* data are listed in Table 3.

The Chen et al. (1985) Δ*UBV* data were obtained during 1985 with the Fernbank Observatory 0.9 m telescope and Yunnan Observatory 1 m telescope. They acquired 140 observations per bandpass of primary eclipse at Fernbank and about 350 data points per bandpass of secondary eclipse at Yunnan. Both data sets used BD +431017 and BD +431016 as the comparison and check stars, respectively.

Table 2
KR Per Spectroscopic Orbital Elements and Related Parameters

Parameter	Value
P (days)	0.9960780 ± 0.0000029
T_0 (HJD)	2,458,146.9330 ± 0.0006
e	0.0 (adopted)
K_1 (km s^{-1})	149.33 ± 0.45
K_2 (km s^{-1})	150.62 ± 0.45
γ (km s^{-1})	−9.71 ± 0.26
$a_1 \sin i$ (10^6 km)	2.0453 ± 0.0060
$a_2 \sin i$ (10^6 km)	2.0630 ± 0.0061
$m_1 \sin^3 i$ ($M_\odot$)	1.3985 ± 0.0093
$m_2 \sin^3 i$ ($M_\odot$)	1.3865 ± 0.0092
Standard error of an observation of unit weight (km s^{-1})	3.6

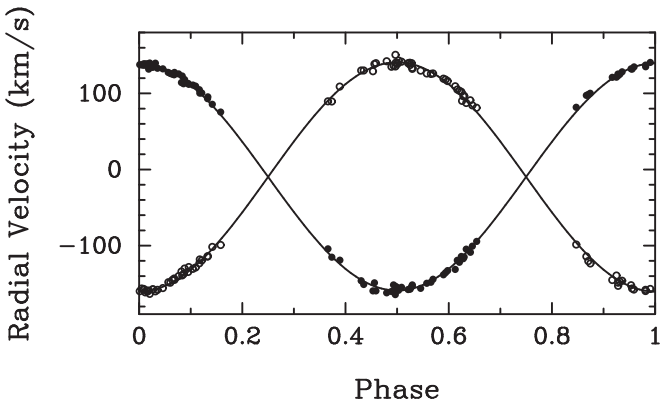

Figure 1. KR Per radial velocities (solid circle = primary; open circle = secondary) compared with the computed velocity curves (solid line). Phase zero is a time of maximum velocity of the primary.

5. Combined Light and Velocity Solution

The 2015 version of the Wilson–Devinney (WD) program was used to determine the combined light and velocity solution. The physical model of that program is described in detail in Wilson & Devinney (1971), Wilson (1979, 1990, 2012a, 2012b), Wilson et al. (2010), Van Hamme & Wilson (2007), and Wilson & Van Hamme (2014). All observations in each data set were assigned a weight of unity. The curve-dependent weights were computed from the standard deviations listed in Table 4. Light level-dependent weights were applied inversely proportional to the square root of the light level. Because of the F5 V combined spectral type and the similar nature of the components, we assumed that the outer envelopes of both stars are convective; consequently, we used the corresponding gravity darkening, g, and bolometric albedo, A, coefficients from Lucy (1967). The two-reflections option (Wilson 1990) was employed, as was the square-root limb-darkening law with the x, y coefficients from Van Hamme (1993). The values of our non-varying parameters are provided in Table 5.

Chen et al. (1985) concluded that the components of KR Per do not fill their Roche lobes, so we analyzed the system using mode 2 of the WD program, which is for detached systems. We adopted the orbital elements from our final spectroscopic solution as starting values for our combined WD solution. We assumed both components rotate synchronously and used solar metal abundances. Our adopted surface temperature of 6500 K for the primary star is based on two considerations. First, Chen et al. (1985) reported a private communication from

Table 3
KR Per Photometric Observations from Emory University

HJD−2,400,000	ΔB	HJD−2,400,000	ΔV	HJD−2,400,000	ΔR	HJD−2,400,000	ΔI
54031.7982	−0.968	54031.7989	−0.886	54031.7994	−0.873	54031.8008	−0.848
54031.8054	−0.936	54031.8061	−0.852	54031.8066	−0.829	54031.8070	−0.821
54031.8113	−0.902	54031.8120	−0.827	54031.8124	−0.803	54031.8129	−0.785
54031.8172	−0.870	54031.8178	−0.792	54031.8183	−0.766	54031.8187	−0.749
54031.8230	−0.831	54031.8237	−0.756	54031.8241	−0.731	54031.8246	−0.706

(This table is available in its entirety in machine-readable form.)

Table 4
KR Per Measurement Characteristics

Observatory	Data Type	Data Points	Norm. Mag.[a]	Std. Dev.[b]
Fernbank	Johnson U	140	−0.0670	0.011
Fernbank	Johnson B	140	−0.0280	0.007
Fernbank	Johnson V	140	+0.0380	0.007
Yunnan	Johnson U	343	−0.0914	0.023
Yunnan	Johnson B	355	−0.0393	0.018
Yunnan	Johnson V	348	+0.0357	0.015
Emory	Johnson B	383	−1.1025	0.009
Emory	Johnson V	379	−1.0201	0.010
Emory	Johnson R	377	−0.9878	0.007
Emory	Johnson I	140	−0.9745	0.007
Fairborn	RV_1	93	⋯	3.3 km s^{-1}
Fairborn	RV_2	93	⋯	3.6 km s^{-1}

Notes.
[a] Magnitude used to normalize the delta magnitudes.
[b] For the light curves, in units of total light at phase 0.25.

Table 5
KR Per Non-varying WD Parameters

Parameter	Symbol	Value
Albedo (bol)	A_1, A_2	0.500, 0.500
Gravity darkening	g_1, g_2	0.300, 0.300
Limb darkening (bol)	x_1, y_1	+0.116, +0.603
Limb darkening (bol)	x_2, y_2	+0.116, +0.603
Limb darkening (U)	x_1, y_1	+0.250, +0.677
Limb darkening (U)	x_2, y_2	+0.250, +0.677
Limb darkening (B)	x_1, y_1	+0.303, +0.580
Limb darkening (B)	x_2, y_2	+0.303, +0.580
Limb darkening (V)	x_1, y_1	+0.115, +0.687
Limb darkening (V)	x_2, y_2	+0.115, +0.687
Limb darkening (R)	x_1, y_1	+0.002, +0.709
Limb darkening (R)	x_2, y_2	+0.002, +0.709
Limb darkening (I)	x_1, y_1	−0.062, +0.678
Limb darkening (I)	x_2, y_2	−0.062, +0.678

W. Bidelman who gave a spectral class of F5 and examined Strömgren indices that supported an F5 V spectral type. Second, from the conversion of the Tycho photometry (Hog et al. 2000) to Johnson values listed in SIMBAD, $V = 10.86 \pm 0.09$ mag and $B = 11.38 \pm 0.10$ mag, the resulting $(B - V) = 0.52$ mag. But with a Gaia/DR2 distance of 376 pc (Gaia Collaboration et al. 2018), there is certainly significant reddening. From the work of Green et al. (2015), we derived $E(B - V) = 0.08$ mag, which gives $B - V = 0.44$ mag. This corresponds to an effective temperature of 6541 K from Flower (1996) while the calibration of Eker et al. (2018) results in 6445 K. Given the reddening correction and the differences in the $(B - V) - T_{\rm eff}$ scales, we estimate an effective temperature uncertainty of ±200 K.

Chen et al. (1985) derived an orbit having a small eccentricity of about 0.009. While this solution fit the Fernbank and Yunnan data well, it did not provide a good match with the more recent Emory photometry and radial velocity data. Our initial spectroscopic solutions of the primary and secondary resulted in very small eccentricities of less than 0.02. Because of the short period of nearly one day, the lines of the components are broad and very weak leading to velocity standard deviations of about 3.5 km s^{-1} from the orbital fits. Thus, the small eccentricities found for the orbits are consistent with a circular orbit. As noted earlier, the theoretical expectation as well as observational results for such short-period systems argue that the orbit should be circular, and so we adopted a zero eccentricity orbit.

Chen et al. (1985) had solutions of the U and B light curves suggesting the system might have a third light contribution, so we obtained WD solutions with that parameter enabled. The results indicated no third light in the Emory and Fernbank data. The possibility of third light in the Yunnan was borderline given the size of the error bars. We proceeded with the assumption of no third light.

A slightly varying period was noted by Chen et al. (1985). The advantage of the 2015 WD program is it can include times of minimum (TOM) dates in addition to the photometric and spectroscopic observations. Table 2 from Chen et al. (1985) lists TOMs for visual, photographic, and photoelectric observations. We made use of only their photoelectric measurements of primary eclipse. We searched the literature for more recent TOMs, and we computed two TOMs from the Emory data. We eventually compiled a total of 25 photoelectric or CCD photometry values (see Table 6), covering the years 1999 to 2015. The weights given in the table are based on the reciprocal of the provided measurement error. All but two of these TOMs are for primary eclipse.

An $O - C$ diagram of the 23 photoelectric TOMs of primary eclipse is presented in Figure 2. It utilizes the ephemeris of Chen et al. (1985) and shows that the trend appears to be linear but the slope is not horizontal; hence, the period needs to be refined. We determined a better period and epoch, but even with these new values the fit of the computed light curve solutions through the data sets was not satisfactory. The inclusion of a linearly changing period (dP/dt) was a significant improvement, but there were still poor fits in certain phase ranges. The WD program does not have a non-linear variable period option, so we decided to use phases instead of HJDs. We determined epochs and periods for each of the four photometric and radial velocity data sets, and then computed the corresponding phases. Due to the large number of years

Table 6
KR Per Photoelectric Times of Minima

TOM HJD−2,400,000	Uncertainty HJD−2,400,000	Eclipse	Weight	Source
45311.7181	⋯	Pri	100	Chen et al. (1985)
45323.6712	⋯	Pri	100	Chen et al. (1985)
45324.6668	⋯	Pri	100	Chen et al. (1985)
45324.6670	⋯	Pri	100	Chen et al. (1985)
45324.6672	⋯	Pri	100	Chen et al. (1985)
45351.5614	⋯	Pri	100	Chen et al. (1985)
51512.3087	0.0002	Pri	100	Agerer et al. (2001)
52712.5783	0.0006	Pri	1	Dvorak (2004)
52957.6093	0.0006	Pri	1	Dvorak (2004)
52966.5746	0.0006	Pri	1	Dvorak (2004)
52983.5074	0.0003	Pri	100	Hübscher (2005)
53387.4165	0.0005	Sec	4	Hübscher et al. (2005)
53682.7549	0.0001	Pri	900	Nelson (2006)
53746.50230	⋯	Pri	900	Brát et al. (2007)
53759.45287	⋯	Pri	900	Brát et al. (2007)
53780.3702	0.0003	Pri	100	Hübscher (2007)
54506.5109	0.0008	Pri	2	Hübscher et al. (2009)
54555.31831	0.0006	Pri	3	Brát et al. (2008)
54555.31991	0.0012	Pri	1	Brát et al. (2008)
54555.32011	0.0008	Pri	2	Brát et al. (2008)
54827.2473	0.0001	Pri	900	Hübscher et al. (2010)
55453.77905[a]	0.0001	Pri	900	This study
55471.70848[a]	0.0001	Pri	900	This study
57060.4507	0.0003	Pri	100	Hübscher (2015)
57354.789	0.002	Sec	1	Nelson (2016)

Notes. Except for the two secondary eclipse TOM, these HJDs were used in Figure 2.
[a] The TOM was determined with a simultaneous solution of the $\Delta BVRI$ data.

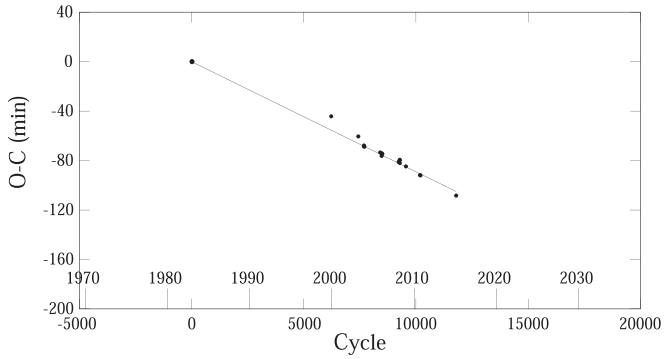

Figure 2. An $O - C$ diagram of photoelectric and CCD primary eclipse times of minima for KR Per from the literature (see Table 6). The ephemeris based on the least-squares fit is (Min I) = HJD 2445,311.7180 ± 0.0001 + 0.9960776 ± 0.0000001E. The previous period given by Chen et al. (1985) was 0.9960838 ± 0.0000041.

spanned by the Emory observations, the linear period change option was necessary. The resulting individual epochs, periods, and dP/dt terms are listed in Table 7.

Our WD solution using the entire set of data reveals that the two components have almost identical characteristics. The masses are $M_1 = 1.466 \pm 0.015 M_\odot$ and $M_2 = 1.458 \pm 0.015 M_\odot$, and the equal-volume radii are $R_1 = 1.855 \pm 0.021 R_\odot$ and $R_2 = 1.824 \pm 0.022 R_\odot$ for the primary and secondary, respectively. The inclination is $82\overset{\circ}{.}36 \pm 0\overset{\circ}{.}04$ and the orbit was assumed to be circular. A listing of all the WD solution parameters is given in Table 8, and the absolute dimensions are in Table 9. Figures 3–5 plot the Fernbank, Yunnan, and Emory observations for each filter set of data along with the light curve solutions. Figures 6–8 are the corresponding plots of the residuals.

Both components of KR Per are found to be slightly nonspherical. The WD program computes geometrical sizes of the two stars. Relative radii are given in four directions: from the center toward the poles, toward the sides, toward the back, and toward the point. The relative radii are listed in Table 10. Figure 9 shows the relative shapes and orbital separation at phase 0.25. The image contains an overlay of the Roche lobes, which was computed by utilizing the mode 6 (contact binary) option of the WD program with the final solution. The primary and secondary stars have filled their Roche lobes by 82% and 81%, respectively.

6. Discussion

Our WD analysis of the nearly identical components of KR Per produces uncertainties of better than 3% for its masses and radii. Thus the KR Per system joins the list of over 90 detached eclipsing binaries with masses and radii with similar uncertainties that was compiled by Torres et al. (2010). Given the nearly identical effective temperatures of the components and their position on the main sequence in the H–R diagram as shown below, we adopt F5 V spectral types for both components.

A couple of the eclipsing binaries in the list of Torres et al. (2010) have very similar characteristics to our computed values for KR Per. For example, both components of RZ Cha are F5 V stars and have surface temperatures of 6450 K and masses of 1.49 $M_\odot$. However, the components of RZ Cha have radii of 2.26 $R_\odot$, and so they are somewhat more evolved than

Table 7
WD Ephemerides Parameters for KR Per Data Sets

Observatory	Epoch	Period	dP/dt
Fernbank	$2445324.66622 \pm 0.11 \times 10^{-3}$	$0.99607819 \pm 0.06 \times 10^{-6}$	...
Yunnan[a]	$2445324.66323 \pm 0.16 \times 10^{-3}$	$0.99603990 \pm 0.13 \times 10^{-6}$	...
Emory	$2455471.70856 \pm 0.08 \times 10^{-3}$	$0.99607976 \pm 0.13 \times 10^{-6}$	$0.36 \times 10^{-9} \pm 0.16 \times 10^{-9}$
Fairborn[b]	$2458147.18080 \pm 0.60 \times 10^{-3}$	$0.9960780 \pm 2.9 \times 10^{-6}$	...

Notes.
[a] Epoch was determined by treating the observations as primary eclipse data, and then subtracting half of the period.
[b] Period from spectroscopic solution (see Table 2) was assumed.

Table 8
KR Per Light and Velocity Curve Results[a]

Parameter	Symbol	Value
Eccentricity	e	0.0[b]
Systemic velocity (km s^{-1})	γ	-9.73 ± 0.36
Semimajor axis ($R_\odot$)	a	6.003 ± 0.016
Inclination (deg)	i	82.357 ± 0.036
Mass ratio	M_2/M_1	0.9949 ± 0.0036
Surface potential	Ω_1	4.272 ± 0.019
Surface potential	Ω_2	4.326 ± 0.021
Temperature (K)	T_1	6500[b]
Temperature (K)	T_2	6482 ± 4
Luminosity ratio in U (Fernbank)	$L_1/(L_1+L_2)_U$	0.514 ± 0.007
Luminosity ratio in U (Yunnan)	$L_1/(L_1+L_2)_U$	0.514 ± 0.007
Luminosity ratio in B (Emory)	$L_1/(L_1+L_2)_B$	0.514 ± 0.007
Luminosity ratio in B (Fernbank)	$L_1/(L_1+L_2)_B$	0.514 ± 0.007
Luminosity ratio in B (Yunnan)	$L_1/(L_1+L_2)_B$	0.514 ± 0.007
Luminosity ratio in V (Emory)	$L_1/(L_1+L_2)_V$	0.513 ± 0.006
Luminosity ratio in V (Fernbank)	$L_1/(L_1+L_2)_V$	0.513 ± 0.006
Luminosity ratio in V (Yunnan)	$L_1/(L_1+L_2)_V$	0.514 ± 0.007
Luminosity ratio in R (Emory)	$L_1/(L_1+L_2)_R$	0.513 ± 0.006
Luminosity ratio in I (Emory)	$L_1/(L_1+L_2)_I$	0.512 ± 0.006

Notes.
[a] WD simultaneous solution, including proximity and eclipse effects, of the light and velocity data.
[b] Adopted value, see Section 5 in the text.

Table 9
Fundamental Parameters of KR Per

Parameter	Primary	Secondary
$M\,(M_\odot)$	1.466 ± 0.015	1.458 ± 0.015
$R\,(R_\odot)$	1.855 ± 0.021	1.824 ± 0.022
$L/L_\odot$	5.53 ± 0.81	5.29 ± 0.78
M_{bol} (mag)	2.89 ± 0.36	2.94 ± 0.37
$\log g$ (cm s^{-2})	4.07 ± 0.01	4.08 ± 0.01
T (K)	6500[a]	6482 ± 4

Note.
[a] Adopted value, see Section 5 in the text.

the components of KR Per. For DM Vir, both of its stars have surface temperatures of 6500 K but are classified as F7 V. Their masses are 1.45 $M_\odot$ and the radii are 1.76 $R_\odot$. Although Allen (2000) lists magnitudes of 3.5 mag for F5 V and 4.0 mag for F8 V, the absolute magnitudes for RZ Cha and DM Vir by Torres et al. (2010) are 2.48 and 2.98 mag. This implies the dimensions of KR Per are typical for its mass and surface temperature.

The theoretical analysis of Hut (1981) shows that the timescales for orbital circularization and spin–orbit axial alignment are similar. As noted in Section 2, our measured $v \sin i$ values are 92 ± 3 km s^{-1} for both components. Assuming that the orbital and rotational axes are parallel, the inclination of 82°.36 increases the rotational values to 92.8 km s^{-1}. With our orbital period and radii (see Tables 7 and 9), we compute rotational velocities of 94.2 ± 1.1 km s^{-1} and 92.6 ± 1.1 km s^{-1} for the primary and secondary, respectively. Thus, the components of KR Per appear to be synchronously rotating.

To check on consistency, we compare our derived stellar brightness with the Gaia distance and Tycho magnitudes. First, we computed the M_{bol} values using our temperatures and radii in the Stephan–Boltzman equation (see Table 9). For the error bars, we used the WD radii results and our assumed $\Delta T = \pm 200$ K. The calculated solar luminosities are 5.53 ± 0.81 and 5.29 ± 0.78, and the magnitudes are $M_{bol} = 2.89 \pm 0.36$ mag and $M_{bol} = 2.94 \pm 0.37$ mag for the primary and secondary, respectively. Second, KR Per was observed by Gaia (Gaia Collaboration et al. 2018) but not by Hipparcos (van Leeuwen 2007). The Gaia/DR2 parallax is 0.0026606 ± 0.0000577 arcsec, corresponding to a distance of 375.86 ± 8.16 pc. Utilizing the bolometric correction from Flower (1996) of 0.01 mag for both stars and the Gaia distance, we obtain $V = 10.78 \pm 0.41$ mag and $V = 10.83 \pm 0.41$ mag for the two components. Third, these combine to give a brightness for the system of $V = 10.05 \pm 0.52$ mag. Noting that the converted Tycho (Hog et al. 2000) Johnson V magnitude for KR Per is 10.86 ± 0.09 mag, this indicates that about 0.81 mag of interstellar absorption is required to reconcile the differences between the observed and computed apparent magnitudes. Is this a realistic scenario? The Bayestar19 and Bayerstar17 reddening data (Green et al. 2019, 2017) provide $E(g-r)$ best-fit values of 0.306 mag and 0.072 mag, respectively, for the KR Per galactic coordinates $l = 159°.6281$ and $b = -1°.9946$ and our distance modulus; however, they note this is a region and distance for which they have no stars. Their conversion factor to $E(B-V)$ is 0.884, so the computed range for $E(B-V)$ is from 0.27 down to 0.06 mag. Using $R_V = 3.1$, the resulting absorption values are 0.84–0.19 mag. The maximum of this range provides the necessary interstellar absorption to reconcile the differences.

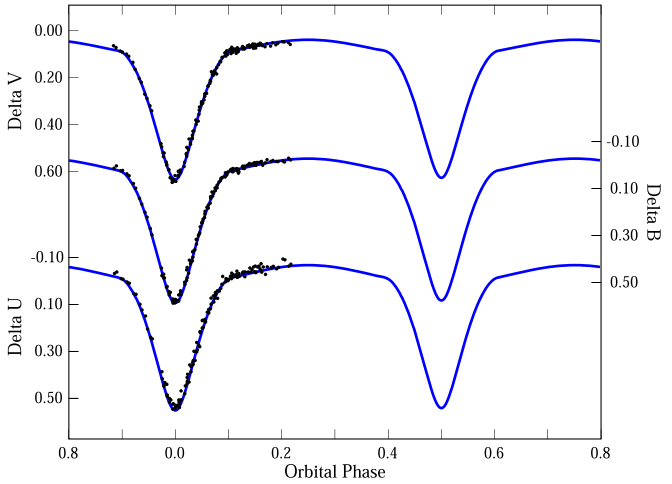

Figure 3. Differential Johnson *UBV* magnitudes of KR Per obtained at the Fernbank Observatory during 1985 by Chen et al. (1985) and fitted with the WD solution curves.

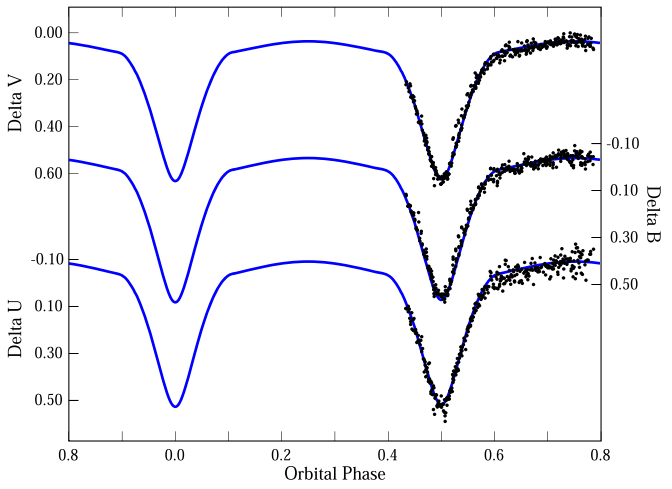

Figure 4. Differential Johnson *UBV* magnitudes of KR Per obtained at the Yunnan Observatory during 1985 by Chen et al. (1985) and fitted with the WD solution curves.

Because the components of KR Per are nearly identical, their properties provide little leverage in testing single-star evolutionary theory. Nevertheless, in a theoretical H–R diagram we compare our results with the stellar evolution tracks from the

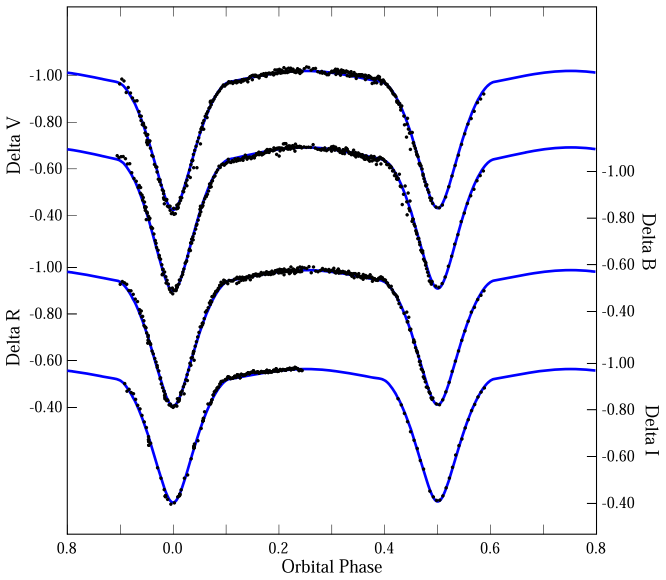

Figure 5. New differential Johnson *BVRI* magnitudes of KR Per acquired at the Emory University Observatory during 2006–2011 and fitted with the WD solution curves.

Yonsei–Yale series (Yi et al. 2001; Demarque et al. 2004) to obtain estimates of the components' abundances and evolutionary status and the age of the system. The best fit for the 1.466 $M_{\odot}$ primary is produced with a metal Z value of 0.022, which corresponds to [Fe/H] = 0.06 (see Table 2 in Kim et al. 2002). The evolutionary tracks for 1.466 $M_{\odot}$ and 1.458 $M_{\odot}$ stars and the absolute dimensions of KR Per are plotted in Figure 10. It shows that the components are still well ensconced on the main sequence. We estimate the system's age as 2.1 $\pm$ 0.1 Gyr.

Binaries with very short periods often are part of multiple systems. Tokovinin et al. (2006) examined a sample of 165 solar-type binaries and found that 96% of those with periods less than 3 days were triple. In their eclipsing binary analysis Chen et al. (1985) suggested that KR Per might have a light contribution from a third component. As noted in Section 5, our WD solutions of the various observatory data sets provide little evidence of third light; however, our analysis does indicate a changing orbital period. Thus, if the system is triple, its third star would need to be very faint or be a low-mass binary itself, and the outer orbital period would be significantly greater than many decades. Additional TOM determinations are certainly warranted.

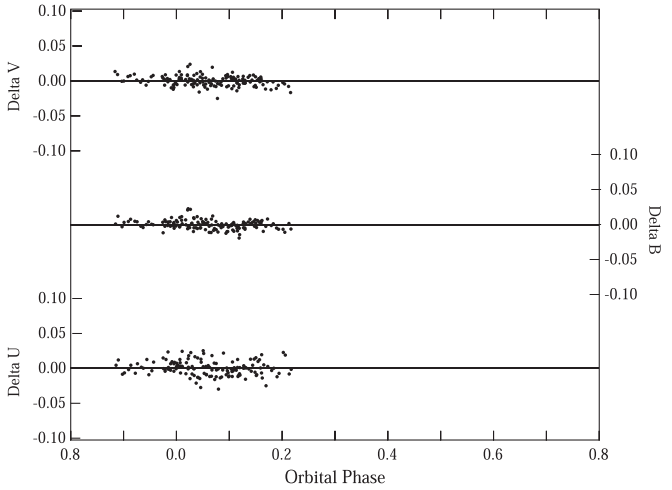

Figure 6. Residuals of the Fernbank *UBV* photometry with respect to the WD solution.

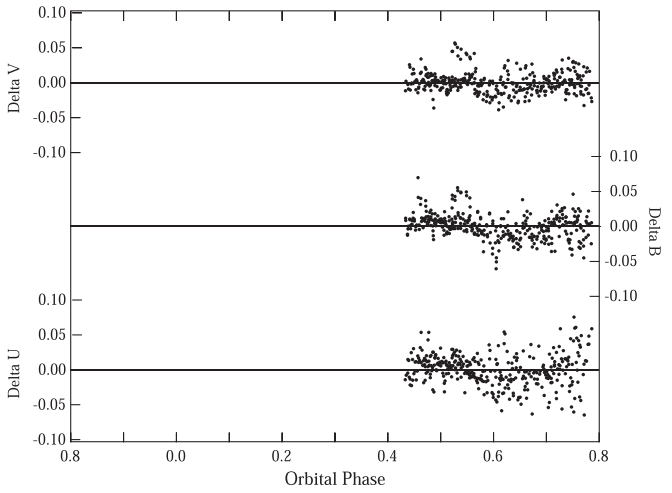

Figure 7. Residuals of the Yunnan *UBV* photometry with respect to the WD solution.

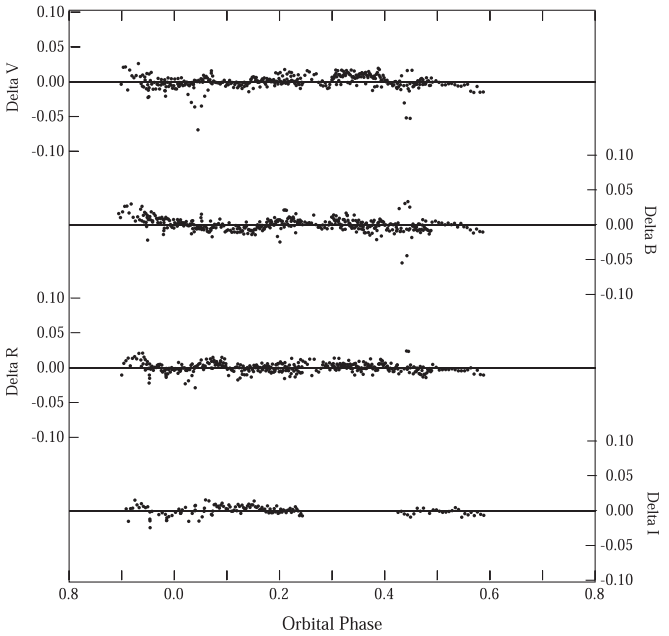

Figure 8. Residuals of the Emory *BVRI* photometry with respect to the WD solution.

Table 10
Model Relative Radii for KR Per

Parameter	Value
r_1 (pole)	0.3010 ± 0.0016
r_1 (point)	0.3327 ± 0.0026
r_1 (side)	0.3097 ± 0.0018
r_1 (back)	0.3227 ± 0.0022
r_2 (pole)	0.2960 ± 0.0020
r_2 (point)	0.3255 ± 0.0031
r_2 (side)	0.3042 ± 0.0022
r_2 (back)	0.3165 ± 0.0026

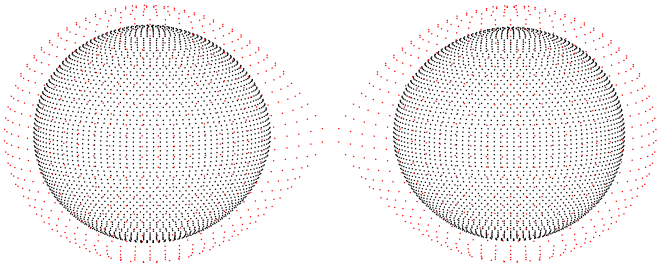

Figure 9. Image of KR Per at phase 0.25. The Roche lobes were computed by utilizing the mode 6 (contact binary) option of the WD program.

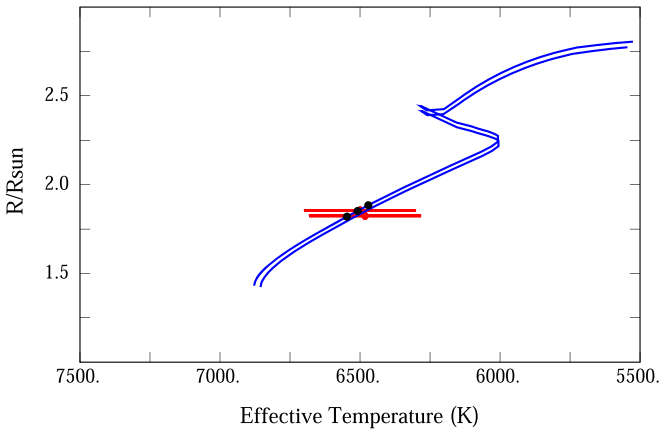

Figure 10. Yonsei–Yale radius vs. temperature evolutionary tracks are shown for 1.466 $M_{\odot}$ to 1.458 $M_{\odot}$ stars, from top to bottom, with $Z = 0.022$ (approximately [Fe/H] = 0.06). The two red points and error bars are the values for the two components. The black dots on the 1.466 $M_{\odot}$ curve indicate ages of 2.0, 2.1, and 2.2 Gyr, respectively. The estimated age is 2.1 ± 0.1 Gyr.

We acknowledge the anonymous referee's criticisms and suggestions, for these greatly improved the results we now present. We continue to again thank Walter Van Hamme (Florida International University) for discussions about the WD program's various aspects. Astronomy at Tennessee State University is supported by the state of Tennessee through its Centers of Excellence program. Our research made use of the SIMBAD database, operated by CDS in Strasbourg, France. This work also made use of data from the European Space Agency (ESA) mission Gaia (https://www.cosmos.esa.int/gaia), processed by the Gaia Data Processing and Analysis Consortium (DPAC, https://www.cosmos.esa.int/web/gaia/dpac/consortium). Funding for the DPAC has been provided by national institutions, in particular the institutions participating in the Gaia Multilateral Agreement.

ORCID iDs

James R. Sowell https://orcid.org/0000-0003-3480-0957
Francis C. Fekel https://orcid.org/0000-0002-9413-3896
Jeffrey L. Coughlin https://orcid.org/0000-0003-1634-9672

References

Agerer, F., Dahm, M., & Hübscher, J. 2001, IBVS, 5017, 1
Allen, C. W. 2000, in Allen's Astrophysical Quantities, ed. A. N. Cox (4th ed.; London: Athone Press), 388
Barker, E. S., Evans, D. S., & Laing, J. D. 1967, RGOB, 130, 355
Brát, L., Šmelcer, L., Kučáková, H., et al. 2008, OEJV, 94, 1
Brát, L., Zejda, M., & Svoboda, P. 2007, OEJV, 74, 1
Chen, K.-Y., Williamon, R. M., Liu, Q., Yang, Y., & Lu, L. 1985, AJ, 90, 1855
Demarque, P., Woo, J.-H., Kim, Y.-C., & Yi, S. K. 2004, ApJS, 155, 667
Duquennoy, A., & Mayor, M. 1991, A&A, 248, 485
Dvorak, S. W. 2004, IBVS, 5502, 1
Eaton, J. A., & Williamson, M. H. 2004, SPIE, 5496, 710
Eaton, J. A., & Williamson, M. H. 2007, PASP, 119, 886
Eker, Z., Bakis, V., Bilir, S., et al. 2018, MNRAS, 479, 5491
Fekel, F. C., & Griffin, R. F. 2011, Obs, 131, 283
Fekel, F. C., Tomkin, J., & Williamson, M. H. 2009, AJ, 137, 3900
Flower, P. J. 1996, ApJ, 469, 355
Gaia Collaboraton, Brown, A. G. A., Vallenari, A., et al. 2018, A&A, 616, A1
Green, G. M., Schlafly, E. F., Finkbeiner, D. P., et al. 2015, ApJ, 810, 25
Green, G. M., Schlafly, E. F., Finkbeiner, D. P., et al. 2017, MNRAS, 478 651
Green, G. M., Schlafly, E. F., Zucker, C., Speagle, J. S., & Finkbeiner, D. P. 2019, ApJ, 887, 93
Hardie, R. H. 1962, in Astronomical Techniques, Stars and Stellar Systems, ed. W. A. Hiltner, Vol. II (Chicago, IL: Univ. Chicago Press), 178
Hog, E., Fabricius, C., Makarov, V. V., et al. 2000, A&A, 355, L27
Hübscher, J. 2005, IBVS, 5643, 1
Hübscher, J. 2007, IBVS, 5802, 1
Hübscher, J. 2015, IBVS, 6152, 1
Hübscher, J., Lehmann, P. B., Monninger, G., Steinbach, H.-M., & Walter, F. 2010, IBVS, 5918, 1
Hübscher, J., Paschke, A., & Walter, F. 2005, IBVS, 5657, 1
Hübscher, J., Steinbach, H.-M., & Walter, F. 2009, IBVS, 5874, 1
Hut, P. 1981, A&A, 99, 126
Kallrath, J., & Milone, E. F. 2009, Eclipsing Binary Stars: Modeling and Analysis (New York: Springer)
Kim, Y.-C., Demarque, P., Yi, S. K., & Alexander, D. R. 2002, ApJS, 143, 499
Lacy, C. H. S., & Fekel, F. C. 2011, AJ, 142, 185
Lucy, L. B. 1967, ZA, 65, 89
Nelson, R. H. 2006, IBVS, 5672, 1
Nelson, R. H. 2016, IBVS, 6164, 1
Russell, H. N., & Merrill, J. E. 1952, Contributions from the Princeton University Observatory (Princeton, NJ: Princeton Univ. Observatory)
Scarfe, C. D. 2010, Obs, 130, 214
Tokovinin, A., Thomas, S., Sterzik, M., & Udry, S. 2006, A&A, 450, 681
Torres, G., Andersen, J., & Gimenez, A. 2010, A&ARv, 18, 67
Van Hamme, W. 1993, AJ, 106, 2096
Van Hamme, W., & Wilson, R. E. 2007, ApJ, 661, 1129
van Leeuwen, F. 2007, Hipparcos, The New Reduction of the Raw Data, Vol. 350 (Berlin: Springer)
Wilson, R. E. 1979, ApJ, 234, 1054
Wilson, R. E. 1990, ApJ, 356, 613
Wilson, R. E. 2012a, JASS, 29, 115
Wilson, R. E. 2012b, AJ, 144, 73
Wilson, R. E., & Devinney, E. J. 1971, ApJ, 166, 605
Wilson, R. E., & Van Hamme, W. 2014, ApJ, 780, 151
Wilson, R. E., Van Hamme, W., & Terrell, D. 2010, ApJ, 723, 1469
Wolfe, R. H., Horak, H. G., & Storer, N. W. 1967, in Modern Astrophysics, ed. M. Hack (New York: Gordon & Breach), 251
Yi, S. K., Demarque, P., Kim, Y.-C., et al. 2001, ApJS, 136, 417
Zahn, J.-P. 1977, A&A, 57, 383